

Observation of non-Kondo-like electronic structure in strongly correlated electron system YbB₆

M. Neupane*,¹ S.-Y. Xu*,¹ N. Alidoust,¹ G. Bian,¹ D.J. Kim,² Chang Liu,¹ I. Belopolski,¹ T.-R. Chang,³ H.-T. Jeng,^{3,4} T. Durakiewicz,⁵ H. Lin,⁶ A. Bansil,⁷ Z. Fisk,² and M. Z. Hasan^{1,8}

¹*Joseph Henry Laboratory and Department of Physics,
Princeton University, Princeton, New Jersey 08544, USA*

²*Department of Physics and Astronomy, University of California at Irvine, Irvine, CA 92697, USA*

³*Department of Physics, National Tsing Hua University, Hsinchu 30013, Taiwan*

⁴*Institute of Physics, Academia Sinica, Taipei 11529, Taiwan*

⁵*Condensed Matter and Magnet Science Group, Los Alamos National Laboratory, Los Alamos, NM 87545, USA*

⁶*Graphene Research Centre, Department of Physics,
National University of Singapore, Singapore 117542, Singapore*

⁷*Department of Physics, Northeastern University, Boston, Massachusetts 02115, USA*

⁸*Princeton Center for Complex Materials, Princeton University, Princeton, New Jersey 08544, USA*

(Dated: November 12, 2019)

The rare-earth material YbB₆ has been theoretically predicted to be a topological Kondo insulator. Using angle-resolved photoemission spectroscopy, we present a careful study of the electronic structure of YbB₆ which is known to be a doped “semi-conductor” from transport experiments. We show that the lowest f -orbital in YbB₆ is about 1 eV away from the Fermi level suggesting the near-absence of Kondo insulating like behavior in contrast to the well known mixed-valence system SmB₆. Our spectroscopic data show that the Fermi level of YbB₆ features nearly linearly dispersive quasi two-dimensional states without observable out-of-plane momentum k_z dispersion. These states are found to form three disjoint Fermi surface pockets enclosing the time-reversal invariant Kramers’ points projected onto the 2D Brillouin zone. The temperature evolution and photon energy coupling of the states do not reveal any Kondo-like behavior. Guided by the systematic experimental data, we present new band calculations with adjustable correlation parameter (Hubbard- U), which suggest that a parity inversion is possible in this system without a Kondo insulating state or other similar mechanisms. Our experimental and theoretical results taken together provide an intriguing possibility for realizing a topological insulator state in correlated rare-earth electron systems even without a Kondo mechanism in contrast to the SmB₆.

PACS numbers:

Rare-earth materials are interesting because the strong electronic correlation in their f -electrons leads to novel ground states such as a Kondo insulating state, valence fluctuation state, and heavy fermion superconductivity [1–4]. Among these correlation-driven ground states, Kondo insulators are characterized by a particularly narrow band gap (on the order of 10-40 meV) at low temperatures with the chemical potential in the gap. Unlike typical band insulators such as SiO₂, the energy gap that opens up at low temperatures in a Kondo insulator is in fact due to the Kondo hybridization of localized f -electrons with conduction electrons [1–4]. With the advent of topological insulators [5–10], recently the rare-earth Kondo insulator, SmB₆, has attracted much interest due to the theoretical prediction that it exhibits a topological Kondo insulator (TKI) phase [11–13]. In a TKI, the Kondo hybridization between the d and f bands further leads to an inversion of the band parity, and therefore realizes a topologically nontrivial insulator phase. Following the theoretical predictions, photoemission and transport experiments have identified the existence of an odd number of in-gap surface states and a two-dimensional conductance channel at low tempera-

tures in SmB₆ [14–20], consistent with the theoretically predicted TKI phase. However, the surface states in TKI phase of SmB₆ only exist at very low temperatures [15] and their Fermi velocity is expected to be low due to a strong f -orbital contribution [13, 15], limiting its future utilization in devices.

In order to search for other novel correlated topological phases even without a Kondo mechanism, it is quite suggestive to systematically study the electronic ground-states of other rare-earth materials that are closely-related to SmB₆. SmB₆ belongs to a class of materials called the rare-earth hexaborides, RB₆ (R = rare-earth metal). In general, rare-earth hexaboride compounds are known to feature three types of electronic bands in the vicinity of the Fermi level, namely the the rare-earth $5d$ orbital band, the rare-earth $4f$ orbital band, and the boron $2p$ band. The low energy physics for a rare-earth hexaboride is collectively determined by the relative energies between these bands and the Fermi level, which depends on a delicate interplay among the key physical parameters including the valence of the rare-earth element, the lattice constant, the spin-orbit coupling (SOC), etc. Therefore, interestingly, the rare-earth hexaborides can

realize a rich variety of distinct electronic ground states as seen in SmB_6 , YbB_6 , EuB_6 and the superconducting state in LaB_6 ($T_c \sim 0.5$ K) [4, 21, 22]. Recently, it has been theoretically predicted that YbB_6 is a TKI [22].

Despite these interesting aspects, apart from SmB_6 , experimental studies on the electronic groundstates of RB_6 compounds are almost entirely lacking. In this paper, we report systematic studies of the electronic groundstate of another representative member of the rare-earth hexaboride family, ytterbium hexaboride (YbB_6). In contrast to the Kondo insulator state in SmB_6 , YbB_6 is known to be a doped semiconductor from transport experiments [21]. This contrast is particularly interesting since SmB_6 and YbB_6 share many important properties such as the same crystal structure and the same sets of low energy bands (R $5d$, R $5f$, and B $2p$). Moreover, it is interesting to investigate whether the semiconducting state in YbB_6 can also host topological order and how that order is different from that in the TKI phase in SmB_6 . Here, we utilize angle-resolved photoemission spectroscopy (ARPES) to systematically reveal the electronic structure of YbB_6 . We show that unlike in SmB_6 , lowest f -orbital in YbB_6 is about 900 meV away from the Fermi level suggesting the near absence of Kondo insulating behavior in contrast to the well known mixed-valence system SmB_6 . Our spectroscopic data show that the Fermi level of YbB_6 features nearly linearly dispersive states without observable out-of-plane momentum k_z dispersion. These states are found to form three Fermi surface pockets enclosing the time-reversal invariant Kramers' points projected onto the surface Brillouin zone. The temperature evolution and photon energy coupling of the states do not reveal any Kondo-like behavior. Guided by the systematic experimental data, we present new band calculations with an adjustable correlation parameter (Hubbard- U) which suggest that a parity inversion is possible in this system without a Kondo insulating state or other similar mechanisms. Our experimental and theoretical results taken together provide an intriguing possibility for realizing a topological insulator state in rare-earth correlated electron systems even without a Kondo mechanism in contrast to the SmB_6 .

Single crystalline samples of YbB_6 used in our measurements were grown by Al-flux method in the Fisk Lab at University of California (Irvine) which is detailed elsewhere [17, 21]. Synchrotron-based ARPES measurements of the electronic structure were performed at the Synchrotron Radiation Center, Wisconsin, the Advanced Light Source (ALS), Berkeley, and Stanford Radiation Lightsource (SSRL), Stanford equipped with high efficiency R4000 electron analyzers. The energy resolution was set to be 10-30 meV, and the angular resolution was set to be better than 0.2° for all synchrotron measurements. The samples were cleaved along the (001) plane and were measured in ultrahigh vacuum better than 10^{-10} torr. The first-principles electronic structure calculations were performed based on the generalized gradient approximation (GGA) [23] using the pro-

jector augmented-wave method [24, 25] as implemented in the VASP package [26, 27]. The experimental crystallographic structure was used [28] for the calculations. The spin-orbit coupling was included self-consistently in the electronic structure calculations with a $12 \times 12 \times 12$ Monkhorst-Pack k -mesh.

YbB_6 shares the same CsCl type of crystal structure as SmB_6 , as shown in Fig. 1a. The bulk Brillouin zone (BZ) is cubic, where the center of the BZ is the Γ point and the center of each face is the X point. It is known from theoretical calculations [4] that three different atomic orbitals contribute to the low-energy electronic structure, namely the rare-earth $5d$ orbital band, the rare-earth $4f$ orbital band and the boron $2p$ band. Both the valence band maximum and the conduction band minimum are around the X -point [4]. A variety of electronic ground states can be realized due to the delicate interplay of the relative energy levels among these bands and the Fermi level. For example, the left panel of Fig. 1e shows a condition for the Kondo insulator state, as observed in SmB_6 . The R $5d$ and R $4f$ bands cross each other near the Fermi level, whereas the B $2p$ band lies energetically below the $5d$ and $4f$ bands, and therefore is irrelevant to the low-energy physics. At low temperatures, the itinerant $5d$ electrons hybridize with the localized $5f$ electrons and open up a Kondo energy gap, which leads to the Kondo insulating state. On the other hand, the right panel of Fig. 1e presents a different scenario, where the R $4f$ band resides far away from the Fermi level. In this case, the R $5d$ and B $2p$ bands dominate the low-energy physics, and they can even show a finite band inversion depending on details of material parameters. In order to reveal the electronic state of YbB_6 , we systematically study its electronic structure at the (001) natural cleavage surface. Fig. 1c shows the momentum-integrated photoemission spectrum over a wide binding energy window. The Yb $4f$ and Yb $5p$ core levels are clearly observed. To more precisely determine the energy positions of the Yb $4f$ with respect to the Fermi level, we present k -resolved dispersion map. As clearly seen in Fig. 1d, the lowest $4f$ flat band in YbB_6 is 1 eV below the Fermi energy. This is in sharp contrast to the ARPES data on SmB_6 , where the flat $4f$ band is found to be only ≤ 15 meV away from the Fermi level. Therefore, our data reveal the physical origin for the absence of the Kondo insulating state in YbB_6 , which also negates the recent theoretical work that predicts the existence of the topological Kondo insulator phase in YbB_6 [22]. Apart from the intense $4f$ band, our data in Fig. 1d also reveal an electron-like pocket centered at the \bar{X} point that crosses the Fermi level.

In order to systematically resolve the Fermi level electronic structure, in Figs. 2 and 3 we present high-resolution ARPES measurements in the close vicinity of the Fermi level. It is important to note that at the studied (001) surface, the three X points (X_1 , X_2 , and X_3) in the bulk BZ project onto the $\bar{\Gamma}$ point and the two \bar{X} points on the (001) surface BZ, respectively. Since the

valence band maximum and conduction band minimum are at the X -points, at the (001) surface one would expect low energy electronic states near the $\bar{\Gamma}$ point and \bar{X} points. The Fermi surface map of YbB_6 is presented in Fig. 2a. Our Fermi surface map reveals multiple pockets, which consist of an oval-shaped contour and a nearly circular-shaped contour enclosing each \bar{X} and $\bar{\Gamma}$ points, respectively. No pocket is seen around the \bar{M} -point. YbB_6 shows metallic behavior in transport [21] which is consistent with our data.

We present ARPES energy and momentum dispersion maps, where low-energy states consistent with the observed Fermi surface topology are clearly identified. As shown in Fig. 2b, a “V”-shaped nearly linearly dispersive band is observed at each $\bar{\Gamma}$ and \bar{X} points. We further study the photon energy dependence of the observed “V”-shaped bands. As shown in Figs. 2b and 3a, the “V”-shaped bands are found to show no observable dispersion as the incident photon energy is varied, which suggests its quasi two-dimensional state nature. Therefore, our systematic ARPES data has identified three important properties in the YbB_6 electronic structure: (1) An odd number of Fermi surface pockets are observed to enclose the Kramers’ point; (2) The bands at the Fermi level are found to exhibit nearly linearly (Dirac like) in-plane dispersion; (3) No observable out-of-plane (k_z) dispersion is observed for these Dirac like (“V”-shaped) bands. All these properties that we observed seem to suggest a possibility for a topological insulator state in YbB_6 . Nevertheless, it is important to note that if these “V”-shaped bands are indeed the upper Dirac cone part of the topological surface states, then one would also expect the lower Dirac cone part. In our data, some hole-like band (e.g. $E \simeq -0.4$ eV in the first panel of Fig. 3a) is seen that can correspond to the low Dirac cone. The observed hole-like band features are not sharp enough to draw any definitive conclusion. We further test the temperature dependence of these “V”-shaped bands. As shown in Fig. 3b, the “V”-shaped bands are observed to be quite robust as one increases temperature. Some changes of the spectrum as a function of temperature are seen, which we will discuss in a later paragraph.

In order to better understand the electronic structure that we observed in ARPES, we perform first-principle calculations on the bulk band structure of YbB_6 using the GGA + SOC + U method. Fig. 4 shows the calculated YbB_6 bulk band structure obtained by using various on-site U values for the Yb $4f$ orbitals. For $U = 0$, our calculation shows that the Yb $4f$ orbital is located very close to the Fermi level and crosses with the Yb $5d$ band. This is inconsistent with our data, which clearly shows that the lowest $4f$ band is 1eV away from the Fermi level and does not cross the Yb $5d$ conduction band. Thus we study the calculated band structure with nonzero U values. Fig. 4b shows the calculation for $U = 4$ eV. Interestingly, it can be seen that the Yb $4f$ band is moved toward higher energies away from the Fermi level as one increases U . For $U = 4$ eV, the $4f$ band moves to a higher

energy and does not cross the $5d$ band, which agrees with our data. Furthermore, the B $2p$ band is “pushed” toward the Fermi level and form a hole-like valence band, also consistent with our data. A finite band inversion between the Yb $5d$ and B $2p$ bands is obtained from our calculation for $U = 4$ eV. Spin-orbit coupling opens a finite (inverted) energy gap, leading to an inversion of the parity eigenvalues at the X point between the d and p bands. Since there are three distinct X points, the inverted band gap at the X points for $U = 4$ eV suggests a novel scenario for a topological insulator state due to the hybridization between d - p bands.

We discuss a few interesting aspects of our data. First, our systematic data suggest an intriguing possibility for realizing a topological insulator state in rare-earth hexaboride system even without a Kondo mechanism. However, the topological insulator state cannot be conclusively demonstrated based on the current data since the lower Dirac cone part is not well resolved. In order to rigorously show the topological insulator state in YbB_6 , spin-resolved ARPES measurements [29] will also be critical to reveal the spin-momentum locking behavior. Second, qualitative agreement between our calculation and our ARPES data are found only when finite U is used in the calculation. The calculated band structure with $U = 0$ is inconsistent with our data. This fact suggests the important role for on-site Coulomb repulsion in determining the electronic groundstate of YbB_6 . Third, since the d - p hybridization gap in calculation is found to be small (≤ 50 meV), one would expect the in-gap topological surface states lie about at 300 meV below the native Fermi level (Fig. 2b) in a narrow energy range. In this case, the “V”-shaped quasi 2D bands that we observed should be surface and bulk mixed states (as surface states tangentially merge into the bulk bands in $E - k$ space). The clear observation of the predicted d - p hybridization gap (≤ 50 meV) will require ultra-high resolution ARPES measurements at ultra-low temperatures [15]. Fourth, we observe finite changes of the ARPES spectrum as a function of temperature (Fig. 3b). For example, the “V”-shaped band is found to move upward along energy axis with increasing temperature. At $T = 100$ K (third panel in Fig. 3b), it seems like the “V”-shaped band does not touch with the hole-like band features any more. This temperature dependent might be related to the d - p hybridization phenomena in calculation, which becomes much weaker at higher temperatures. Finally, if YbB_6 is indeed a topological insulator due to d - p orbital hybridization, then it would be extremely interesting to study the $\text{Sm}_{1-x}\text{Yb}_x\text{B}_6$ (note that SmB_6 and YbB_6 share the same crystal structure) system, where a number of exotic topological quantum phase transitions, such as topological phase transition from a d - f hybridized topological Kondo insulator phase to a d - p hybridized topological insulator phase, are expected.

In conclusion, by using high-resolution ARPES, we show that unlike SmB_6 , the lowest f -orbital in YbB_6 is about 1 eV away from the Fermi level, which reveals that

it is not a TKI. Our data show that the Fermi level of YbB_6 features nearly linearly dispersive bands without observable out-of-plane momentum k_z dispersion. These bands are found to form odd Fermi surface pockets en-

closing the Kramers' points per BZ [30]. Our results provide an intriguing possibility for realizing a topological insulator state in rare-earth hexaboride systems even without considering the Kondo mechanism.

-
- [1] G. Aeppli and Z. Fisk, *Comm. Condens. Matter Phys.* **16**, 155-165 (1992).
- [2] P. Riseborough, *Adv. Phys.* **49**, 257-320 (2000).
- [3] P. Coleman, *Handbook of Magnetism and Advanced Magnetic Materials* **1**, 95-148 (2007).
- [4] V. N. Antonov *et al.*, *Adv. Con. Mat. Phys.* **2011**, 1-107 (2011).
- [5] M. Z. Hasan and C. L. Kane, *Rev. Mod. Phys.* **82**, 3045-3067 (2010).
- [6] X.-L. Qi and S.-C. Zhang, *Rev. Mod. Phys.* **83**, 1057-1110 (2011).
- [7] L. Fu and C. L. Kane, *Phys. Rev. B* **76**, 045302 (2007).
- [8] D. Hsieh *et al.*, *Nature* **452**, 970-974 (2008).
- [9] Y. Xia *et al.*, *Nat. Phys.* **5**, 398-402 (2009).
- [10] M. Z. Hasan and J. E. Moore, *Ann. Rev. Cond. Mat. Phys.* **2**, 55-78 (2011).
- [11] M. Dzero *et al.*, *Phys. Rev. Lett.* **104**, 106408 (2010).
- [12] T. Takimoto, *J. Phys. Soc. Jpn.* **80**, 123710 (2011).
- [13] F. Lu *et al.*, *Phys. Rev. Lett.* **110**, 096401 (2013).
- [14] N. Xu *et al.*, *Phys. Rev. B* **88**, 121102(R) (2013).
- [15] M. Neupane *et al.*, *Nat. Commun.* **4**, 2991 (2013).
- [16] J. Jiang *et al.*, *Nat. Commun.* **4**, 3010 (2013).
- [17] S. Wolgast *et al.* *Phys. Rev. B.* **88**, 180405(R) (2013).
- [18] D. J. Kim *et al.*, *Nat. Mat.* **13**, 466470 (2014).
- [19] D. J. Kim, *et al.*, *Sci. Rep.* **3**, 03150 (2013).
- [20] X. Zhang *et al.*, *Phys. Rev. X* **3**, 011011 (2013).
- [21] J. M. Tarascon *et al.*, *Appl. Phys. Lett.* **100**, 253115 (2012).
- [22] H. Weng *et al.*, *Phys. Rev. Lett.* **112**, 016403 (2014).
- [23] P. Perdew, *Phys. Rev. Lett.* **77**, 3865 (1996).
- [24] P. E. Blochl, *Phys. Rev. B* **50**, 17953 (1994).
- [25] G. Kresse, and D. Joubert, *Phys. Rev. B* **59**, 1758 (1999).
- [26] G. Kresse and J. Hafner, *Phys. Rev. B* **48**, 13115 (1993).
- [27] G. Kress, and J. Furthmuller, *J. Comput. Mater. Sci.* **6**, 15 (1996);
- [28] P. P. Blum, and E. F. Beraut, *Acta Cryst.* **7**, 81-84 (1954).
- [29] D. Hsieh *et al.*, *Nature* **460**, 1101-1105 (2009).
- [30] These results of YbB_6 have been presented in APS March Meeting, Denver, Co, 2014. See <http://absuploads.aps.org/presentation.cfm?pid=10894>.

Acknowledgements

The work at Princeton and Princeton-led synchrotron x-ray-based measurements and the related theory at Northeastern University are supported by the Office of Basic Energy Sciences, US Department of Energy (grants DE-FG-02-05ER46200, AC03-76SF00098 and DE-FG02-07ER46352). H.L. acknowledges the Singapore National Research Foundation for the support under NRF Award No. NRF-NRFF2013-03. T.R.C. and H.T.J. are supported by the National Science Council, Taiwan. H.T.J. also thanks NCHC, CINC-NTU and NCTS, Taiwan, for

technical support. T.D. at LANL acknowledges support from Department of Energy, Office of Basic Energy Sciences, Division of Material Sciences, and LANL LDRD program. We also thank M. Hashimoto and S.-K. Mo for beamline assistance at the DOE supported Stanford Synchrotron Radiation Lightsource and the Advanced Light Source (ALS-LBNL) in Berkeley. We thank M. Bissen and M. Severson for beamline assistance at SRC, WI. M.Z.H. acknowledges Visiting Scientist support from LBNL, Princeton University and the A. P. Sloan Foundation.

Correspondence and requests for materials should be addressed to

M.Z.H. (Email: mzhasan@princeton.edu).

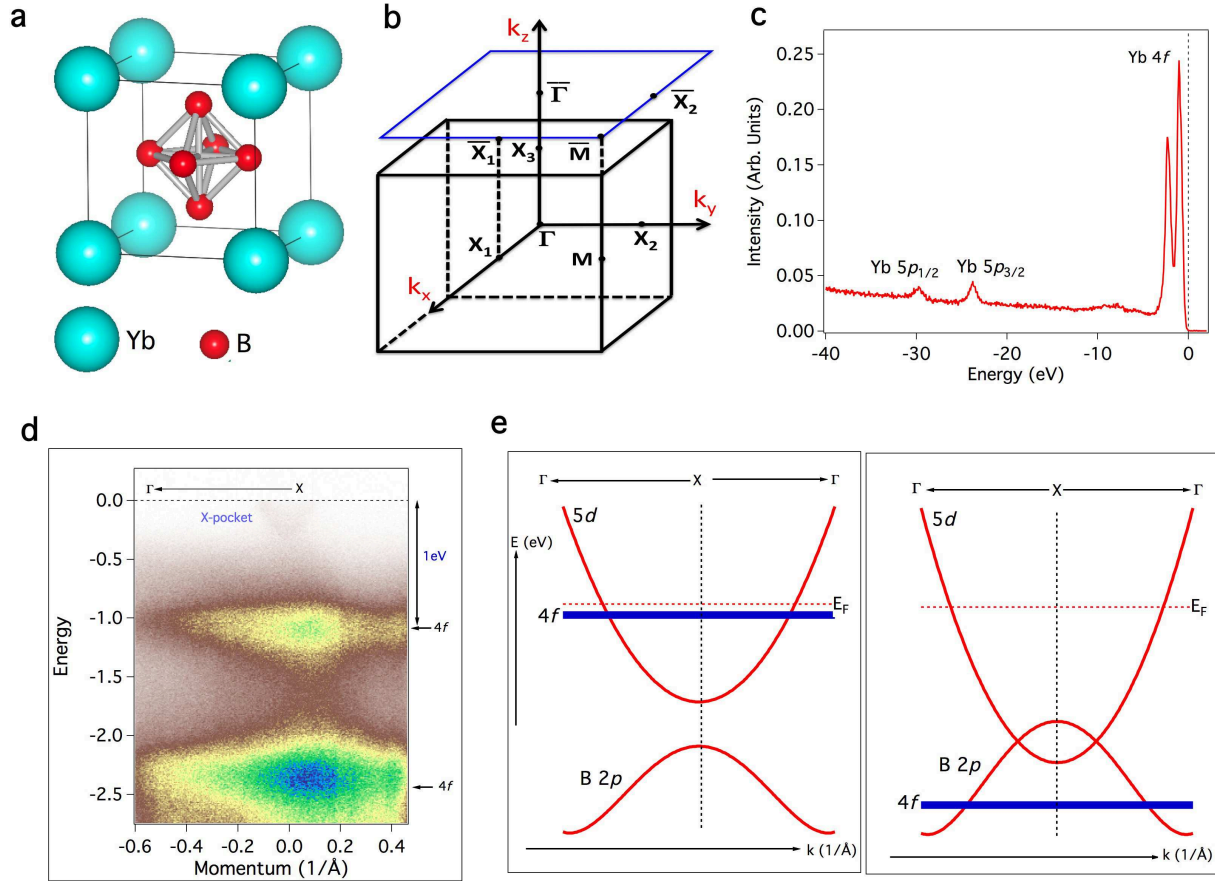


FIG. 1: **Brillouin zone symmetry and band structure of YbB₆.** **a**, Crystal structure of YbB₆. Yb ions and B₆ octahedron are located at the corners and the center of the cubic lattice structure. **b**, The bulk and surface Brillouin zones of YbB₆. High-symmetry points are marked. **c**, Core-level spectroscopic measurement of YbB₆. Various energy levels are marked on the curve. **d** ARPES measured dispersion maps along the $\bar{\Gamma} - \bar{X} - \bar{\Gamma}$ momentum-space cut-directions. Dispersive cone like pocket and non-dispersive flat Yb 4f bands are observed. **e** Different types of possible electronic ground state in rare-earth hexaborides.

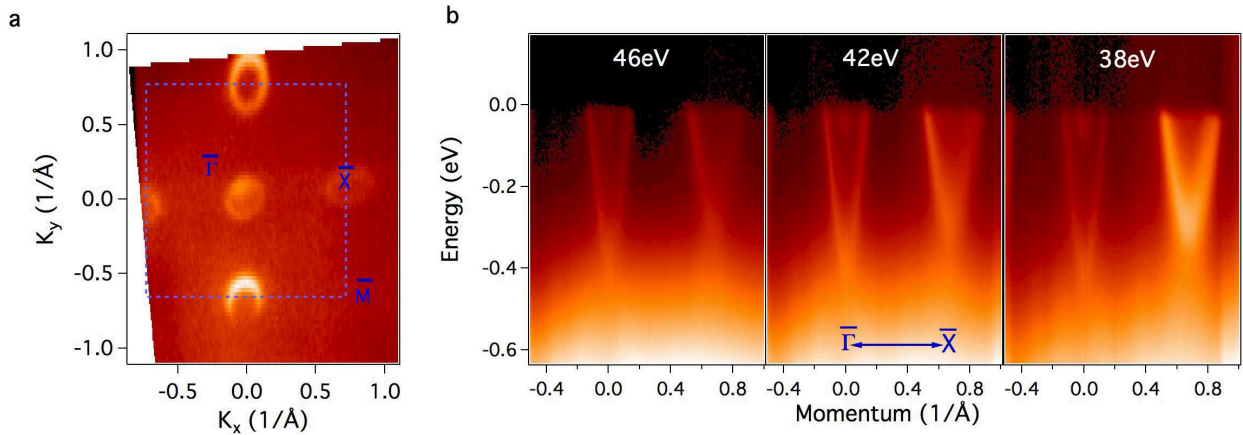


FIG. 2: **Fermi surface and dispersion map.** **a**, ARPES measured Fermi surface of YbB₆. Circular shaped pockets are observed at $\bar{\Gamma}$ and \bar{X} points. It is measured with photon energy of 50 eV at temperature of 15 K. **b**, ARPES dispersion maps measured with different photon energy. The measured photon energy are noted on the plots. These data were collected at ALS BL10.

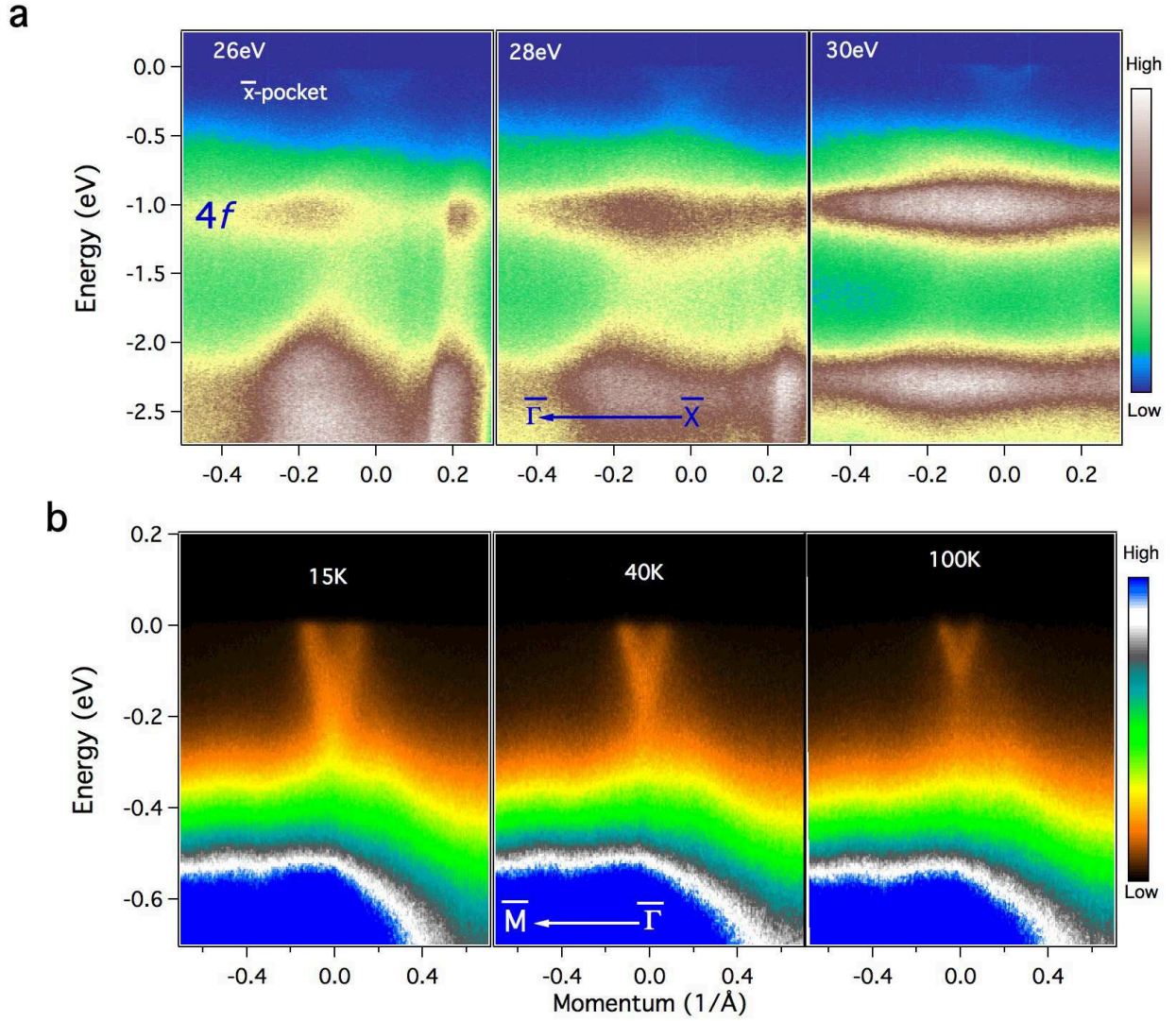


FIG. 3: **Photon energy and temperature dependent dispersion maps** **a**, Photon energy dependent dispersion map with wider binding energy. The measured photon energy are noted on the plots. The $4f$ flat bands are about 1 eV below the Fermi level. These spectra are measured along the $\bar{\Gamma} - \bar{X}$ momentum space cut direction with temperature of 15K . **b**, Temperature dependent ARPES spectra. The measured temperature are noted on the plots. The slight variation of the pocket with temperature is attributed with the thermal expansion of the sample. These spectra are measured along the $\bar{\Gamma} - \bar{M}$ momentum space cut direction. These data were collected at SRC PGM beamline.

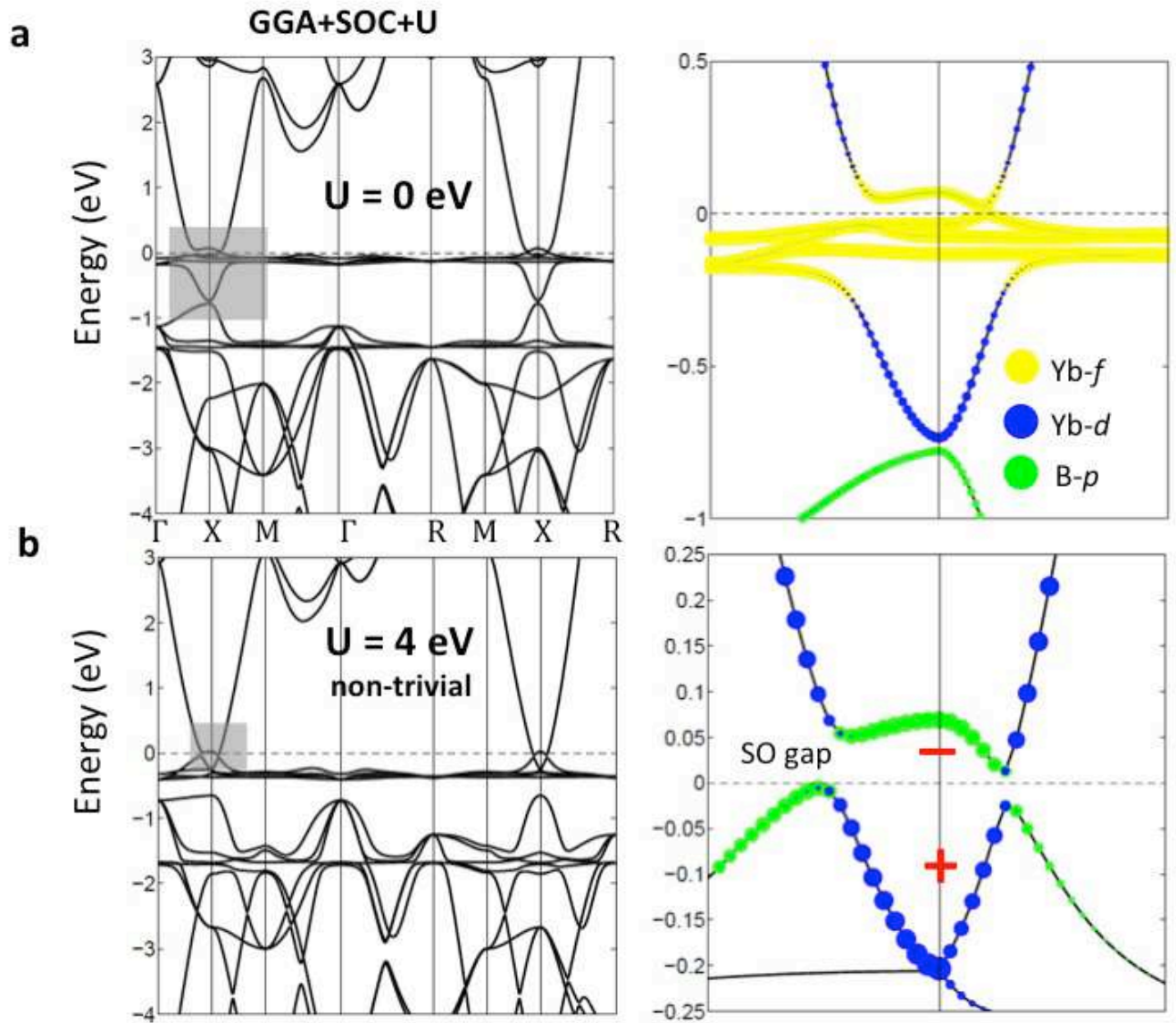


FIG. 4: **First-principle electronic structure of YbB₆.** **a**, Theoretical bulk band structure along different high-symmetry points with on site Coulomb repulsion $U = 0$ eV. At $U = 0$, the *f* bands are closer to the Fermi level (see Fig a, right). **b**, Same as **a** but with $U = 4$ eV, which shows the hybridization between *d* and *p* bands at *X* point and consequently the gap is opened (see Fig b, right). The + and - signs show the parity eigen values of the bands at *X* point, where a band inversion is found.